Journal of NeuroVirology, 7: 409–420, 2001
 ISSN 1355–0284/01 $12.00+.00

CD8-deficient SJL mice display enhanced susceptibility to Theiler's virus infection and increased demyelinating pathology

Wendy Smith Begolka, Lia M Haynes, Julie K Olson, Josette Padilla, Katherine L Neville, Mauro Dal Canto, Joann Palma, Byung S Kim, and Stephen D Miller

Department of Microbiology-Immunology and Interdepartmental Immunobiology Center, Northwestern University Medical School, Chicago, Illinois, USA

Theiler's murine encephalomyelitis virus (TMEV) infection of the central nervous system (CNS) induces a chronic, progressive demyelinating disease in susceptible mouse strains characterized by inflammatory mononuclear infiltrates and spastic hind limb paralysis. Our lab has previously demonstrated a critical role for TMEV- and myelin-specific $CD4^+$ T cells in initiating and perpetuating this pathology. It has however, also been shown that the MHC class I loci are associated with susceptibility/resistance to TMEV infection and persistence. For this reason, we investigated the contribution of $CD8^+$ T cells to the TMEV-induced demyelinating pathology in the highly susceptible SJL/J mouse strain. Here we show that β2M-deficient SJL mice have similar disease incidence rates to wild-type controls, however β2M-deficient mice demonstrated earlier onset of clinical disease, elevated *in vitro* responses to TMEV and myelin proteolipid (PLP) epitopes, and significantly higher levels of CNS demyelination and macrophage infiltration at 50 days post-infection. β2M-deficient mice also displayed a significant elevation in persisting viral titers, as well as an increase in macrophage-derived pro-inflammatory cytokine mRNA expression in the spinal cord at this same time point. Taken together, these results indicate that $CD8^+$ T cells are not required for clinical or histologic disease initiation or progression in TMEV-infected SJL mice. Rather, these data stress the critical role of $CD4^+$ T cells in this capacity and further emphasize the potential for $CD8^+$ T cells to contribute to protection from TMEV-induced demyelination. *Journal of NeuroVirology* (2001) **7,** 409–420.

Keywords: β2-microglobulin; CD8; Theiler's virus; demyelination; multiple sclerosis

Introduction

Although the etiology of multiple sclerosis (MS),[1] an immune-mediated demyelinating disease of the central nervous system (CNS) in humans, remains largely unknown, several lines of evidence suggest the potential for a virus as the initial causative agent (Kurtzke, 1993; Waksman, 1995). Theiler's murine encephalomyelitis virus (TMEV) is a member of the *Picornaviridae* family that induces a chronic progressive demyelinating pathology that closely resembles MS in susceptible strains of mice following

Address correspondence to Stephen D Miller, PhD, Department of Microbiology-Immunology, Northwestern University Medical School, 303 E. Chicago Avenue, Chicago, IL 60611, USA. E-mail: s-d-miller@northwestern.edu

Received 5 April 2001; revised 7 May 2001; accepted 29 May 2001.

[1]Abbreviations: CNS, central nervous system; CTL, cytolytic/cytotoxic T lymphocyte; DTH, delayed-type hypersensitivity; KO, knock-out; MS, multiple sclerosis; OVA, ovalbumin; p.i., postinfection; PLP, proteolipid protein; TMEV-IDD, Theiler's murine encephalomyelitis virus-induced demyelinating disease; β2M, β2-microglobulin.

intracerebral inoculation. TMEV-induced demyelinating disease (TMEV-IDD) is characterized clinically by an abnormal waddling gait resulting from an ascending hind limb spastic paralysis, and histologically by the presence of perivascular inflammatory mononuclear infiltrates within the CNS that result in primary demyelination (Lipton and Dal Canto, 1979; Miller and Karpus, 1994).

It is believed that the mechanisms involved in the development of demyelination involve both direct and bystander immune-mediated processes as evidenced by the presence of inflammatory $CD4^+$ and $CD8^+$ T cells and macrophages within the target organ (Lipton *et al*, 1984; Pope *et al*, 1996), and to a lesser extent, direct viral damage of oligodendrocytes and microglia due to persistent viral infection (Rodriguez *et al*, 1983; Graves *et al*, 1986; Rodriguez *et al*, 1988; Ohara *et al*, 1990). However, the exact nature of these immune effector responses and their contribution to disease pathogenesis is still a matter of some controversy. There is considerable evidence from our own lab, as well as others, that indicates a critical role for $CD4^+$ Th1 cells in mediating both the initial and chronic pathogenesis of TMEV-IDD in the susceptible SJL/J strain, as demonstrated by antibody depletion studies (Rodriguez *et al*, 1986a; Friedmann *et al*, 1987; Welsh *et al*, 1987), the correlation of delayed-type hypersensitivity (DTH) responses with the severity of disease (Miller *et al*, 1997), and the increasing amounts of $CD4^+$ Th1-derived pro-inflammatory cytokines expressed in the CNS throughout disease progression (Begolka *et al*, 1998). Despite these significant findings, there also exist numerous lines of often contradictory evidence from similar studies conducted in resistant C57BL/6 mice with gene deletions to additionally support the role of $CD8^+$ T cells, not only in viral clearance and protection but also in promoting the demyelinating process (Rodriguez *et al*, 1986a; Rodriguez and Sriram, 1988; Fiette *et al*, 1993; Pullen *et al*, 1993; Njenga *et al*, 1996; Murray *et al*, 1998).

Therefore, in this study we sought to definitively establish the effector role of $CD8^+$ T cells in the highly susceptible SJL/J mouse, by utilizing mice which are deficient in the expression of β2-microglobulin (β2M), which fail to positively select any $CD8^+$ T cells (Koller *et al*, 1990; Zijlstra *et al*, 1990). Our results clearly indicate, in correlation with our previous data in this system, that $CD8^+$ T cells fail to provide a significant and demonstrable effector contribution to either the initiation or progression of TMEV-IDD clinical pathology or demyelination. In addition, our data also convincingly demonstrates that the absence of $CD8^+$ T cells leads to an accelerated and more severe disease phenotype, as measured clinically, histologically, and by several *in vitro* parameters, leading to the conclusion that the role of $CD8^+$ T cells is primarily for protection and/or regulation in this system. These data are consistent with our ongoing model for the SJL/J mouse wherein persistent CNS infection with TMEV leads to the continual activation and clonal expansion of TMEV-specific, and eventually neuroantigen-specific, $CD4^+$ Th1 effector cells capable of secreting proinflammatory cytokines and chemokines. These proinflammatory molecules in turn lead to the recruitment and eventual accumulation of activated macrophages/microglia within the CNS resulting in demyelination via a nonspecific bystander response.

Results

Accelerated onset and increased clinical severity of TMEV-IDD in β2M-deficient mice Wild-type SJL and β2M-deficient mice were monitored for the development of clinical signs of demyelination following infection with TMEV (Figure 1). Although the incidence rate for developing TMEV-IDD was not statistically distinct between the two groups (93.1% vs 75.8%), β2M-deficient mice developed a heightened disease phenotype as measured by several parameters. β2M-deficient mice had an accelerated disease onset when compared to control mice (MDO = 29.89 vs 35.08; $P = .038$), and a rapidly progressing chronic disease that was dramatically increased in severity over controls from day 32 postinfection (p.i.) throughout the measured clinical course.

The increased disease severity in the β2M-deficient mice was also evident from gross CNS histology at day 50 p.i. (Figure 2), showing large numbers of perivascular and parenchymal inflammatory infiltrates, which appear to be comprised primarily of

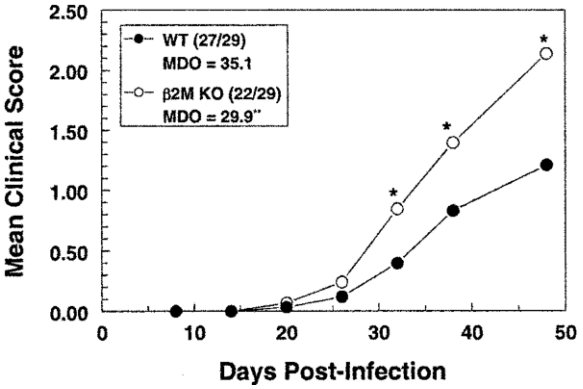

Figure 1 Comparison of clinical disease course between TMEV-infected β2M-deficient SJL mice and wild-type SJL controls. TMEV-IDD was induced in all mice using the BeAn strain of virus and animals were graded for clinical signs as described in Materials and Methods. Results are expressed as mean clinical score of affected animals vs days p.i. from three pooled experiments. Disease scores at 32, 38, and 48 days p.i. are significantly increased in β2M-deficient vs controls as measured by the Mann-Whitney test ($*P < .006$). Mean day of clinical onset (MDO) is also accelerated in β2M-deficient mice ($**P = .038$). No significant difference is observed in the disease incidence rate between β2M-deficient mice (22/29—75.9%) and the wild-type controls (27/29—93.1%) as measured by χ^2 using Fisher's exact test ($P = .1443$).

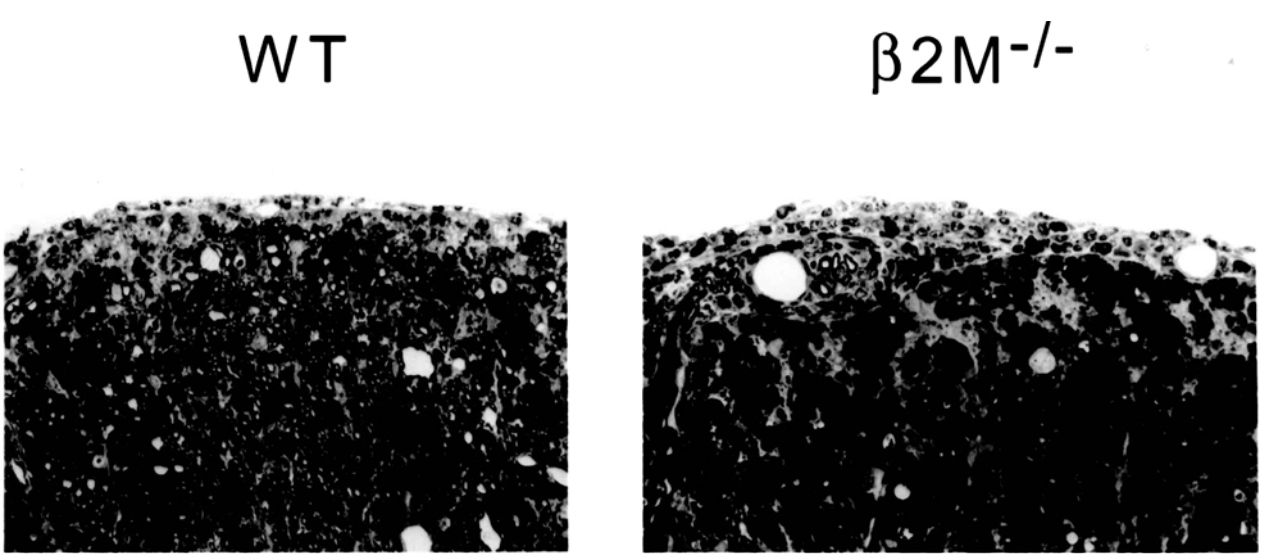

Figure 2 Spinal cord histology of TMEV-infected β2M-deficient SJL and wild-type SJL control mice. Two mice from each group were sacrificed by perfusion on day 50 p.i., and 10 1-μm-thick sections from the lumbar region of the spinal cord were stained with toluidine blue and examined by light microscopy for evidence of inflammatory infiltrate and demyelination. Pathologic changes were graded as follows: **–**, no disease; +/**–**, meningeal inflammation; +, focal parenchymal inflammation with demyelination; ++, multiple areas of parenchymal inflammation and demyelination; +++, extensive inflammation and demyelination with confluent lesions. Shown is representative section for each group of mice, with the wild-type SJL receiving an overall score of +, and the β2M-deficient SJL receiving an overall score of +++.

myelin debris-containing macrophages, as well as extensive white matter demyelination, compared to the milder perivascular CNS damage in wild-type controls. To address if there were qualitative and/or quantitative changes in the nature of the inflammatory infiltrate between the two groups, we also performed immunohistochemistry for CD4, CD8, and F4/80 infiltrates. The increased CNS infiltrates in the β2M-deficient mice were largely the result of accumulation of F4/80$^+$ macrophages/microglia, rather than CD4$^+$ effector cells which were fairly equivalent between wild-type and β2M-deficient mice (Figure 3). As expected, staining for CD8$^+$ T cells was detected in the wild-type infected CNS, albeit at low levels, yet completely absent in β2M-deficient mice, confirming their phenotype. Isotype-matched controls for each antibody as well as staining of CNS tissue from naïve mice revealed no positive cells for any of the three tested markers (data not shown).

Increased viral persistence in the CNS of TMEV-infected β2M-deficient mice While the clinical and histological disease was exacerbated in the β2M-deficient mice, it was also of interest to determine if the severe disease pathology could be attributed to alterations in viral clearance within the CNS due to the lack of cytolytic CD8$^+$ T cells. Viral plaque assays of brain and spinal cord tissue from TMEV-infected β2M-deficient mice at day 50 p.i. revealed a 2–2.5-fold increase in viral titer from both the brain and spinal cord as compared to the wild-type control mice (Figure 4A). Overall, higher levels of virus were isolated from the spinal cord in both groups correlating with the previous observation that TMEV persists to a higher level in this CNS tissue at later time points in disease (Lipton *et al*, 1984). As expected, homogenized kidney samples from both TMEV-infected groups failed to yield any detectable plaques (data not shown). Semiquantitative RT-PCR from spinal cord samples at this same time point also demonstrated an increase in mRNA levels for the TMEV capsid proteins VP1 and VP3 as seen in the plaque assays (Figure 4B). This data illustrates the critical role of the CD8$^+$ T cell in the highly susceptible SJL mouse in regulating levels of infectious virus, and not in contributing to the TMEV-IDD demyelinating pathology.

T cell responses to both TMEV and myelin epitopes are increased in β2M-deficient mice The data to this point indicate that the clinical presentation of TMEV-IDD differs dramatically in the presence or absence of CD8$^+$ T cells in the SJL host, and that in β2M-deficient mice the exacerbated disease severity may be attributed to the pronounced inflammatory infiltrate and increased viral titer. We next sought to determine if the pattern of peripheral immune reactivity to TMEV and myelin proteins, as measured by both *in vivo* and *in vitro* assays was altered between the β2M-deficient and control mice, and thereby provide additional evidence of a contributing mechanism for the observed accelerated disease. Delayed-type hypersensitivity (DTH) analysis of TMEV-infected β2M-deficient at day 50 p.i. demonstrated no significant difference in the level of *in vivo* reactivity to either UV-inactivated TMEV, the immunodominant VP2 70-86 capsid protein peptide, or the immunodominant myelin epitope PLP139-151 when compared to the wild-type infected controls (Figure 5). This does

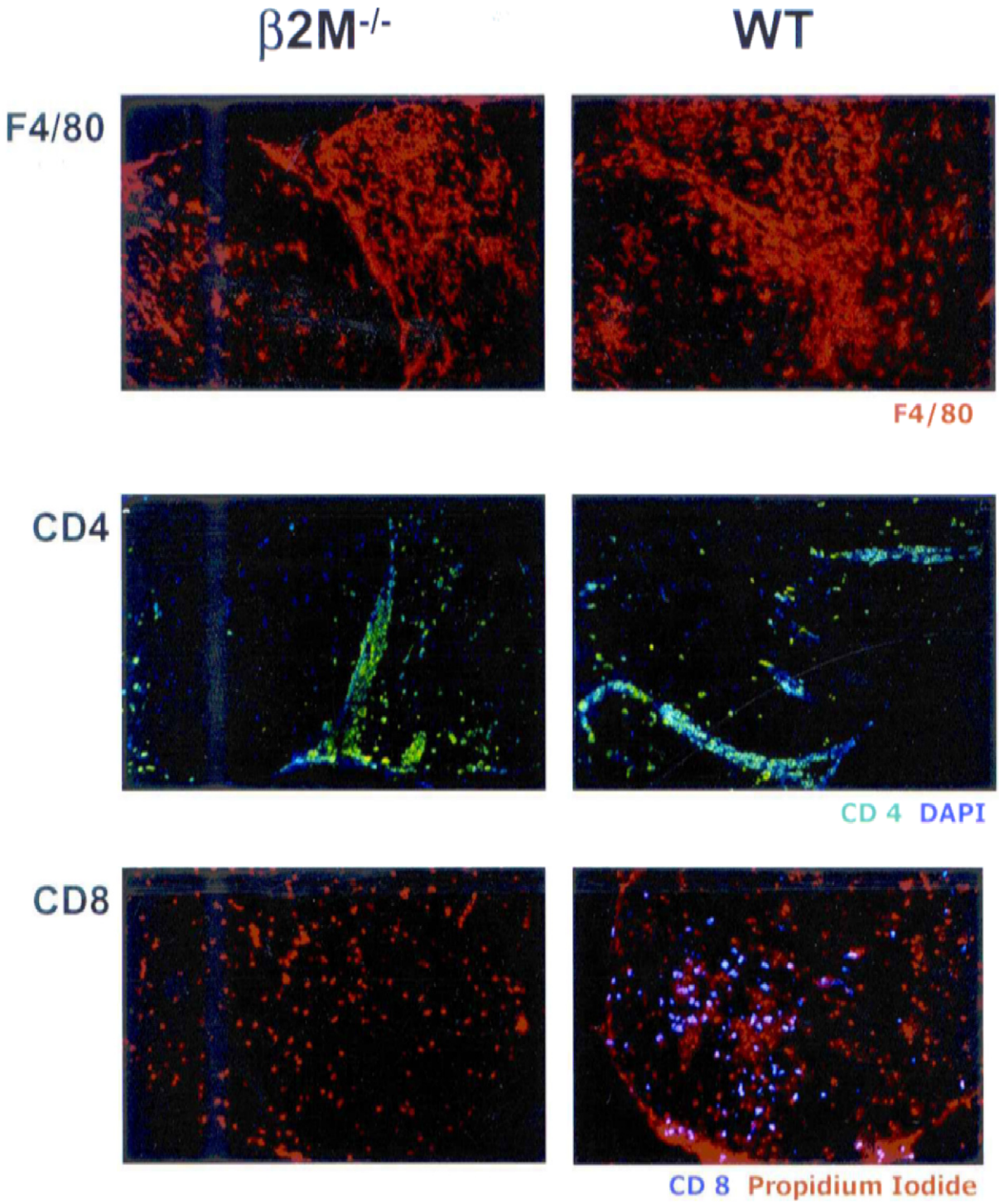

Figure 3 Immunohistochemical staining for $CD4^+$ and $CD8^+$ T cells, and $F4/80^+$ macrophages/microglia in the spinal cords of wild-type and β2M-deficient SJL mice with TMEV-IDD. Spinal cord sections from mice from day 50 p.i. were stained for expression of CD4, CD8, and F4/80 as described in Materials and Methods. Shown is a representative section from each group of mice for each cell surface marker. In the top panels F4/80 staining is shown in red; in the middle panels, CD4 staining is shown in green with a blue DAPI counterstain; and, in the bottom panels, CD8 staining is shown in blue with red propidium iodide counterstain. Magnification is 100×. Isotype-matched control antibody did not stain spinal cords from affected mice, nor was any positive staining revealed in the spinal cords of naïve mice (data not shown).

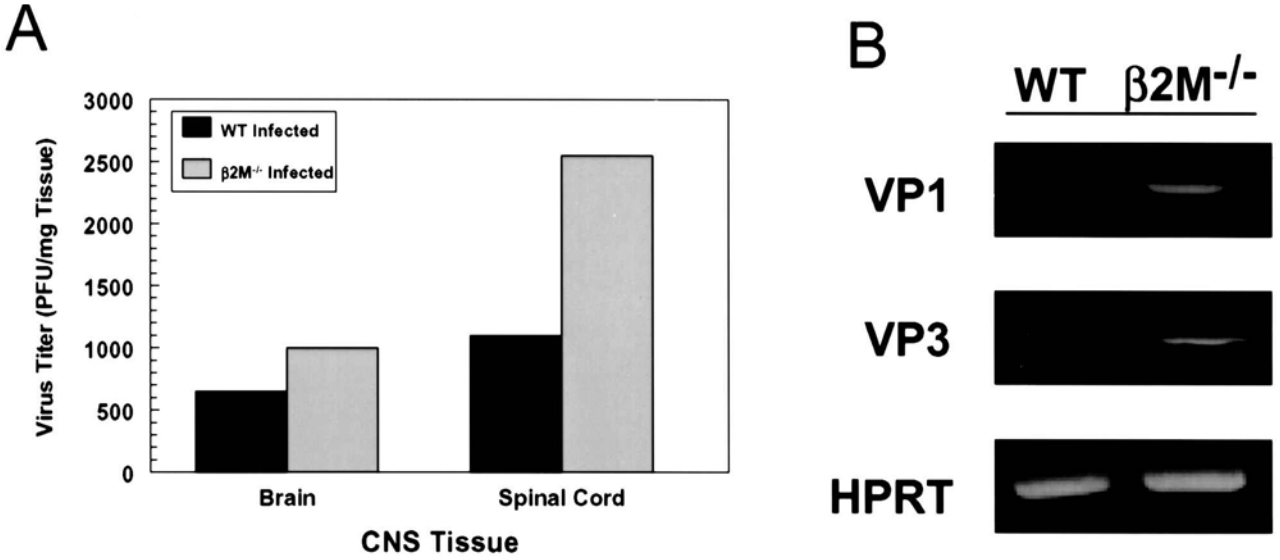

Figure 4 Increased viral titers and mRNA for viral proteins are found in the brain and spinal cord of TMEV-infected β2M-deficient SJL mice. In panel A, three mice at day 60 p.i. from each group were sacrificed, and brain, spinal cord, and kidney (not shown) were isolated, pooled, and processed for a viral plaque assay as described in Materials and Methods. Viral plaques in a BHK monolayer were counted over a series of four dilutions of tissue lysate, with the data shown as the mean PFU (plaque forming unit) per mg of brain and spinal cord starting tissue. Control kidney lysate did not yield any viral plaques. These results are representative of two separate experiments. In panel B, spinal cord-derived RNA from mice at day 60 p.i. was used as a template for semi-quantitative RT-PCR for the TMEV viral capsid proteins VP1 (495bp) and VP3 (445bp).

indicate, however, that β2M-deficient mice are fully competent in developing and sustaining a $CD4^+$ Th1-mediated response.

Although this observation is interesting, it is also possible that we may have missed an accelerated activation and expansion of PLP139-151-specific T cells at the day-50 time point, given that the majority of β2M-deficient mice have already progressed to a severe clinical disease, and may now be displaying enhanced reactivity to additional myelin epitopes not tested. We therefore performed DTH at an earlier time point in disease (day 35 p.i.), and despite yielding similar results for TMEV and VP2 70-86, the β2M-deficient mice now displayed a trend (bordering on significance) toward increased responses to PLP139-151 compared to controls, indicative of accelerated epitope spreading (data not shown).

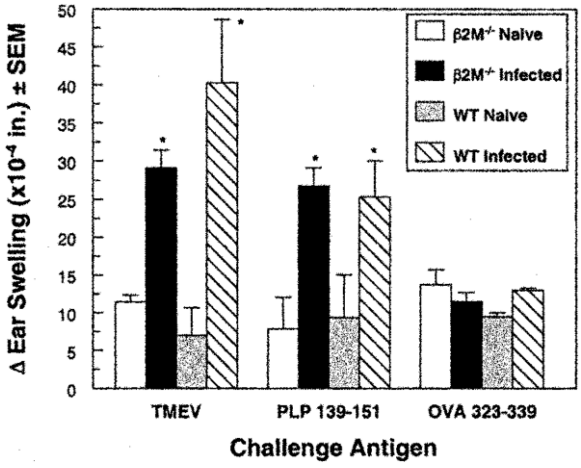

Figure 5 β2M-deficient mice display significant DTH responses to whole TMEV and myelin epitopes. DTH responses to TMEV, PLP139-151, and OVA323-339 were assessed at day 50 p.i. from TMEV-infected β2M-deficient and wild-type control mice (n = 5). The results are expressed as the 24-h ear swelling in units of 10^{-4} inches ± SEM in response to ear challenge with 5 μg UV-inactivated TMEV, 10 μg PLP139-151, or 10 μg OVA323-339. These results are representative of two separate experiments. *DTH responses were significantly greater than uninfected controls as measured by the Student's t-test ($P < .001$).

This trend toward increased neuroantigen reactivity was also observed in the *in vitro* splenic proliferative responses to both viral and myelin epitopes. β2M-deficient mice demonstrated comparable to slightly higher responses, as measured by stimulation indexes, to intact TMEV and VP2 70-86 (Figure 6A), yet dramatically increased reactivity to PLP139-151 (SI = 10.1 vs 3.2) (Figure 6B). Responses to the irrelevant antigen OVA 323-339 were not detected in any experimental group. Given that we have previously demonstrated the ability to detect only low levels of proliferation to this immunodominant epitope at this time point from wild-type animals (Miller *et al*, 1997), collectively these data additionally support the immunological phenomenon of epitope spreading as a contributing factor in the accelerated disease phenotype observed in the β2M-deficient mice.

Increased levels of macrophage-derived proinflammatory mediators in the CNS of β2M-deficient mice With evidence of increased cellular infiltrate, viral titer and cellular responses, we were also

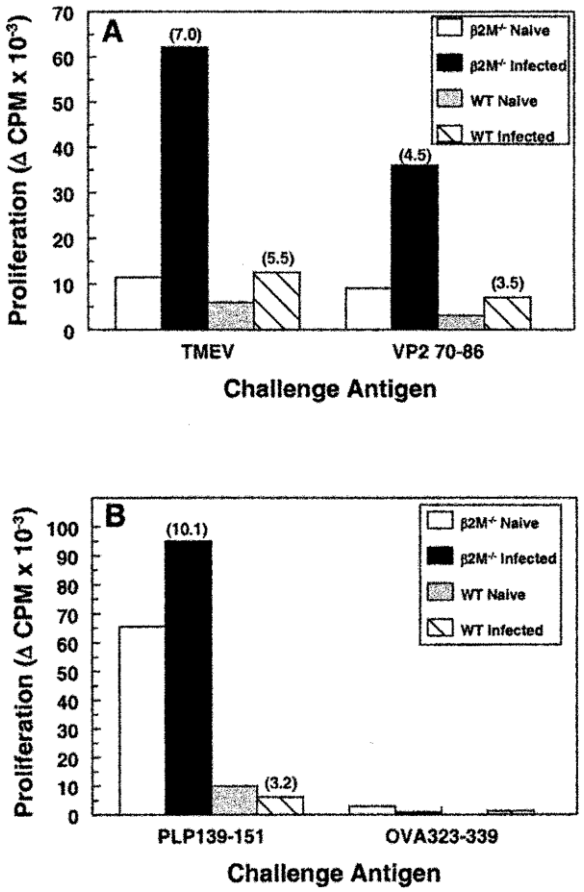

Figure 6 Proliferative responses to TMEV and PLP139-151 are increased in β2M-deficient mice. Splenic cells isolated from TMEV-infected β2M-deficient or wild-type SJL mice 50 days p.i. were cultured with UV-inactivated TMEV and VP2 70-86 (panel A), and PLP139-151 and OVA323-339 (panel B). Data represent the mean ^{3}[H]-thymidine uptake of triplicate cultures stimulated for a total of 96 h with antigen (shown is 5 μg for TMEV and 10 μg for peptides) and is plotted as Δ CPM (no antigen controls subtracted) $\pm$ SEM. Shown above certain results in parentheses are also the proliferation data expressed as the stimulation index (SI = CPM of antigen-containing wells/CPM of control wells). These results are representative of two separate experiments.

interested in the resulting cytokine profile during TMEV-IDD within the CNS of infected animals, as we have previously demonstrated that the levels of mRNA for pro- and anti-inflammatory cytokines continue to increase throughout the disease course in the wild-type SJL mouse (Begolka *et al*, 1998). Any increases in the levels of these cytokines in the β2M-deficient mouse as compared to wild-type would also be indicative of, and contributing to, the observed accelerated disease. Total RNA isolated from mice at day 50 p.i. revealed similar results as the immunohistochemical analysis in Figure 3, demonstrating a 2-fold increase in message for the F4/80 cell surface marker in β2M-deficient mice, but not for CD4, and a concomitant increase in macrophage-derived proinflammatory cytokines such as TNF-α, IL-10, iNOS, and IL-12, without a corresponding increase in comparable cytokines produced by inflammatory CD4$^+$ T cells, as measured by semiquantitative RT-PCR (Figure 7A–C). A notable exception to this for the CD4$^+$ population is the readily detectable increase in IL-4 mRNA, which may be increased as an attempt by the host at intrinsic regulation of a more severe disease pathology.

Discussion

A large body of research has attempted to ascertain whether CD4$^+$ or CD8$^+$ T cells are involved in the initiation, progression and/or regulation of TMEV-IDD. The evidence for CD4$^+$ T cells as mediators of TMEV pathology in susceptible SJL mice is significant in that: 1) monoclonal antibodies against CD4, MHC Class II, or IL-12 either prevented or diminished clinical signs (Friedmann *et al*, 1987; Welsh *et al*, 1987; Inoue *et al*, 1998); 2) flow cytometric and histological data from infected SJL/J mice revealed an increased level of CD4$^+$ T cells and their proinflammatory cytokines during clinical disease progression, and transfer of a CD4$^+$ VP2-specific T cell line leads to increased incidence and accelerated onset of disease (Gerety *et al*, 1994; Pope *et al*, 1996; Begolka *et al*, 1998); 3) the development of virus and myelin antigen-specific DTH corresponds with onset and chronicity of demyelination (Clatch *et al*, 1986; Miller *et al*, 1997); 4) epitopes of TMEV that elicit a Th1 response and DTH can accelerate the pathogenesis of TMEV upon active immunization (Yauch *et al*, 1998); and 5) tolerance via ECDI-coupled cells with TMEV, known to reduce IL-2 and IFN-γ from Th1 cells, reduces the severity of disease (Peterson *et al*, 1993; Karpus *et al*, 1995).

Although these data seem to rigorously support the role of CD4$^+$ Th1 cells in both initiation and progression of TMEV-IDD, there are also a number of published reports suggesting the same is true for CD8$^+$ T cells (Rodriguez *et al*, 1986a; Rodriguez and Sriram, 1988; Matloubian *et al*, 1994; Njenga *et al*, 1996; Murray *et al*, 1998). However, as the majority of these studies were conducted using mice on a resistant genetic background (C57BL/6 and 129/J), in this study we sought to determine the outcome of the TMEV-IDD disease phenotype in the absence of CD8$^+$ T cells in the highly susceptible SJL/J mice that were deficient in the expression of β2M. Previous reports examining the effects of this mutation or the MHC class I knockout counterpart have provided evidence that the absence of CD8$^+$ T cells on the resistant background leads to the establishment of chronic demyelination with or without clinical signs, extensive CNS infiltrate, and high viral titers, leading one to conclude that the primary role of these cells is in protection and regulation of disease (Fiette *et al*, 1993; Pullen *et al*, 1993; Rodriguez *et al*, 1993; Rivera-Quinones *et al*, 1998; Lavi *et al*, 1999). The current results support this central role for CD8$^+$ T cells, with

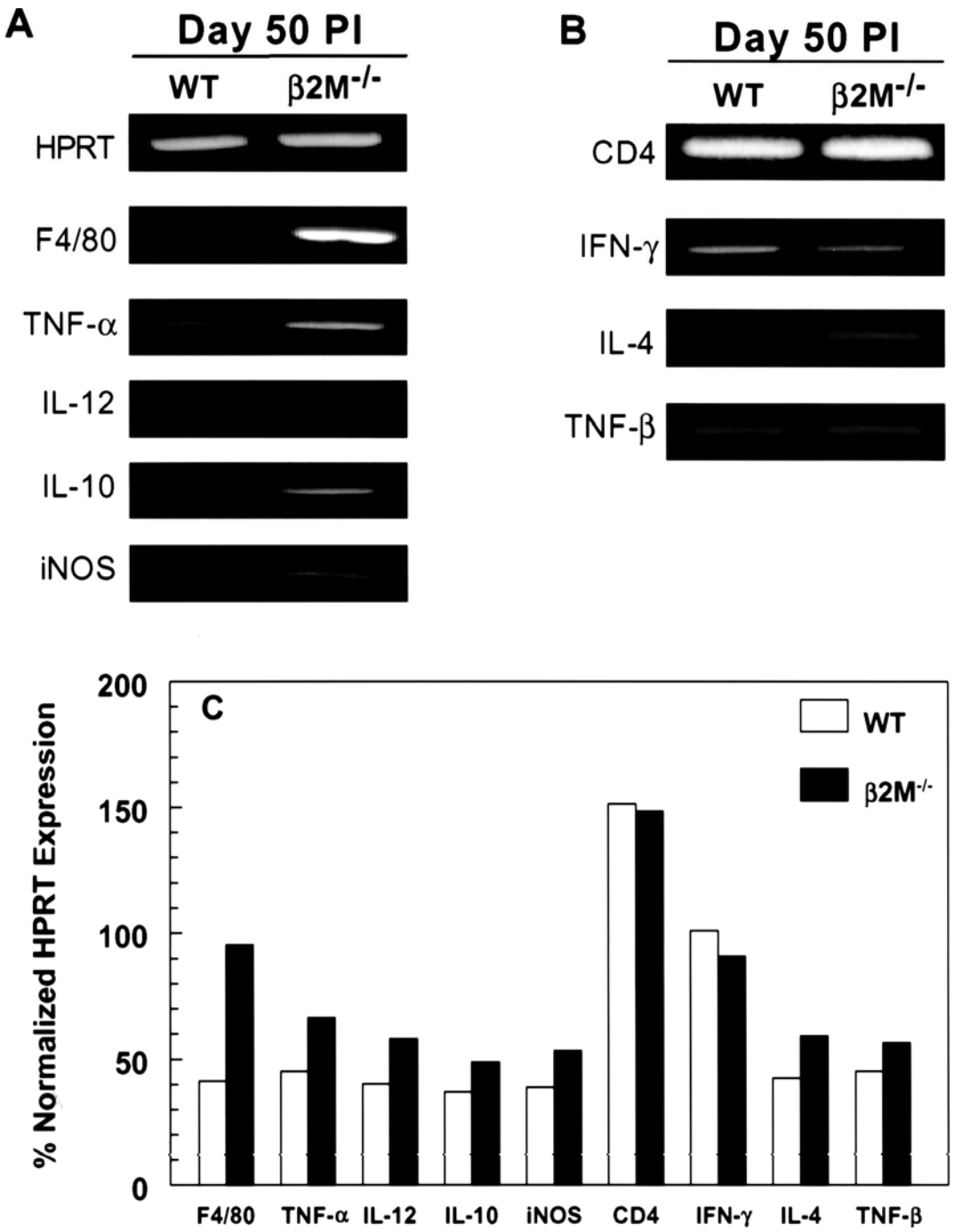

Figure 7 Semiquantitative RT-PCR analysis of cytokine mRNA levels from the spinal cords of TMEV-infected β2M-deficient and wild-type control SJL mice. At 50 days p.i., three mice per group were sacrificed by perfusion and spinal cord RNA was isolated. This total RNA served as the template for RT-PCR as detailed in Materials and Methods. Shown in panel A are the gel images of the amplified products for the control transcript HPRT, the macrophage/microglia cell surface marker F4/80, and the macrophage-derived proinflammatory mediators, TNF-α, IL-12, IL-10, and iNOS. Shown in panel B are the amplified products of the effector T cell marker CD4 and the T cell-derived cytokines IFN-γ, IL-4, and TNF-β (lymphotoxin). Shown in panel C are the densitometry values for the amplified cytokine products in panels A/B following normalization to the housekeeping gene, HPRT. The data are expressed as a percentage of normalized HPRT expression. Results are representative of two separate experiments.

the secondary conclusion that $CD4^+$ effector T cells are sufficient to mediate disease pathogenesis.

First, β2M-deficient mice are highly susceptible to TMEV-IDD, as there was no difference in the incidence rate when comparing them to control mice; however, their progression of disease was remarkable when observing several severity parameters. β2M-deficient mice displayed an accelerated onset of disease, as well as a more severe clinical progression as measured by mean clinical score over the duration of the time course observed. In addition, in one experiment where the mice were allowed to progress to beyond 55 days p.i., 5 out of 11 β2M-deficient mice progressed to a clinical score of 4, with several mice eventually succumbing to the disease by day 60, an observation rarely seen with the wild-type SJL mouse (data not shown). Second, the severe clinical disease in the β2M-deficient mice also correlated with the presence of large numbers of inflammatory infiltrates comprised mainly of activated macrophages/microglia in conjunction with extensive white matter demyelination as compared to the control mice. Expression of cytokine mRNA from the CNS of infected mice additionally confirms the increase in activated macrophage/microglia infiltrate as well as their secreted pro-inflammatory mediators known to promote the $CD4^+$ Th1 environment. Third, β2M-deficient mice were effectively able to mount a specific immune response to both virus and myelin epitopes that was at a minimum equivalent to, yet often exceeded, that of wild-type controls. Last, β2M-deficient mice were significantly hampered in their ability to control viral persistence in both the brain and spinal cord.

Impressively, the current data extend the prior work done with resistant animals to the susceptible SJL/J mouse and confirm the phenotype previously observed. This correlation between outcomes regardless of the genetic background lends strong support to the distinct roles of $CD4^+$ and $CD8^+$ T cells in the TMEV model. Although data indicating the pivotal role of $CD4^+$ T cells in the pathogenesis of TMEV-IDD have been previously reported, an equally compelling body of work also demonstrates the critical role $CD8^+$ T cells play in the control of disease susceptibility. It has been clearly shown that : 1) susceptibility/resistance to TMEV maps to Class I H-2D (Clatch *et al*, 1985; Rodriguez and David, 1985; Rodriguez *et al*, 1986b; Kappel *et al*, 1991); 2) monoclonal antibody depletion of $CD8^+$ T cells leads to earlier onset and increased disease severity (Larsson-Sciard *et al*, 1997); 3) virus-specific CTLs are found at a higher frequency in the CNS of resistant mice than susceptible mice, and *in vivo* IL-2 therapy can effectively boost CTL responses in susceptible strains and diminish viral persistence (Lindsley *et al*, 1991; Pena Rossi *et al*, 1991; Lin *et al*, 1995; Dethlefs *et al*, 1997); 4) perforin KO mice on the normally resistant C57BL/6 background are able to be persistently infected with TMEV (Pena-Rossi *et al*, 1998); and 5) in the BALB/c system, transfer of a $CD8^+$ population from the spleen of TMEV-infected donors protects recipients from disease induction (Nicholson *et al*, 1996; Haynes *et al*, 2000). Taken as a whole, our data in the susceptible SJL/J mouse supplement and are consistent with these previously documented observations and further support a critical role for $CD8^+$ T cells in regulating disease susceptibility and severity.

Our results are, however, in direct contrast with data suggesting $CD8^+$ T cells contribute to the disease pathology of TMEV-IDD (Rivera-Quinones *et al*, 1998; Rodriguez and Sriram, 1988). There are several possible explanations for these observed differences. With regard to the absence of $CD4^+$ T cells leading to an exacerbated disease, the ability to provide cognate B cell to help production of antibody to control the peripheral and CNS viremia is critically impaired (Borrow *et al*, 1993). This is supported by the fact that the anti-TMEV humoral response in susceptible animals is unable to completely clear the virus but is capable of dramatically limiting the spread early in the infection (Lipton and Gonzalez-Scarano, 1978). To that end, CD4-deficient animals die of an overwhelming virally mediated encephalitis within 25 days p.i. (Rodriguez and Sriram, 1988). The depletion of $CD4^+$ T cells in the chronic stages of TMEV-IDD has not been directly addressed in the literature to this point, however, given the compelling evidence for a pathologic role of myelin-specific autoimmunity in chronic disease progression (Miller *et al*, 1997), it is strongly believed that infiltrating $CD4^+$ T cells contribute more significantly to disease progression than its regulation. Our lab has recently addressed this hypothesis through the use of tolerance to a panel of myelin autoepitopes at later time during chronic disease with the observed outcome of diminished clinical score and decreased demyelinating pathology (manuscript submitted). In addition, as it has been demonstrated that susceptible mice are capable of mounting virus-specific CTL responses (Lindsley *et al*, 1991), it is interesting to note that $CD4^+$ T cells have been reported to be required to perpetuate long-term CTL reactivity when infections become persistent, as in the case of LCMV (Matloubian *et al*, 1994).

The observation that the absence of $CD8^+$ T cells leads to a less severe disease is more difficult to reconcile with our data (Rivera-Quinones *et al*, 1998). It is possible that differences related to the strain of virus used (DA vs BeAn) may be a contributing factor, as it has not been completely determined what type of $CD8^+$ responses are elicited during active infection with each strain of virus. It is well documented in both human and mouse that naïve $CD8^+$ T cells are capable of differentiating into Tc1 or Tc2 populations, analogous to Th1 and Th2 cells, depending on the cytokine environment present during initial stimulation (Croft *et al*, 1994; Sad *et al*, 1995; Sad

and Mosmann, 1995; Seder and Le Gros, 1995; Carter and Dutton, 1996). Tc1 development is promoted by IL-18, IL-12, and IFN-γ leading to more of a cytolytic response, whereas Tc2 development is promoted by IL-4 leading to a predominant regulatory response (Li *et al*, 1997). It is possible, then, that in the resistant C57BL/6 strain, where virus is cleared rapidly, that the predominant response is Tc1 in nature. This idea is supported by data indicating that C57BL/6-perforin KO mice are able to be persistently infected with TMEV (Pena-Rossi *et al*, 1998), and that the absence of $CD8^+$ T cells leads to viral titers that are dramatically increased (Figure 4) (Fiette *et al*, 1993; Pullen *et al*, 1993; Rodriguez *et al*, 1993; Rivera-Quinones *et al*, 1998; Lavi *et al*, 1999). This would be in contrast to the susceptible SJL/J strain where the predominant response may be Tc2 in nature, and/or minimally a weak Tc1, and the initial viremia is controlled, but not cleared. These mice, although capable of mounting a cytolytic response during active infection, must be dependent on additional mechanisms to support viral clearance, with the most likely candidate being antibody-dependent responses. This is supported by our observation that the majority of β2M-deficient mice, while displaying an accelerated disease onset and severity of TMEV-IDD, do not succumb to the pathology until after 60 days p.i. Their rapid progression of disease is then most likely a combination of increased viral titer leading to enhanced immune infiltrate and demyelination rather than a virally mediated encephalitis, indicative of a significant regulatory response that is now absent.

Collectively, the current data lend additional support to our model of TMEV-IDD in the susceptible SJL/J mouse wherein persistent CNS infection with TMEV leads to the continual activation and clonal expansion of TMEV-specific, and eventually neuroantigen-specific, $CD4^+$ Th1 effector cells capable of secreting pro-inflammatory cytokines and chemokines. These pro-inflammatory molecules continue to promote an environment favoring Th1 activation, and in turn lead to the additional recruitment and eventual accumulation of activated macrophages/microglia within the CNS resulting in demyelination via a nonspecific bystander response. The role of $CD8^+$ T cells in this model appears to be a combination of both Tc1 cytolytic and Tc2 regulatory responses, but overall they do not appear to contribute significantly to either the demyelinating pathology or the onset of neurological deficit.

Materials and methods

Mice Female SJL/J mice, 6–7 weeks old, were purchased from Harlan Laboratories (Indianapolis, IN). β2M-deficient SJL/J mice were purchased from the Jackson Labs (Bar Harbor, ME). All mice were housed in the Northwestern animal care facility and maintained on standard laboratory chow and water *ad libitum*. Severely paralyzed mice were afforded easier access to food and water.

Peptides PLP139-151(HSLGKWLGHPDKF), OVA 323-339 (ISQAVHAAHAEINEAGR), and VP2 70-86 (WTTSQEAFSHIRIPLP) were purchased from the Peptides International (Louisville, KY). Amino acid composition was verified by laser desorption mass spectroscopy and purity (>98%) was assessed by HPLC.

Induction and clinical evaluation of TMEV-IDD Mice were anesthetized with methoxyflurane (Mallinckrodt Veterinary, Mundelein, IL) and inoculated in the right cerebral hemisphere with (2.9×10^6) plaque-forming units of TMEV, strain BeAn 8386, in 30 μl DMEM. Mice were examined in a single-blinded fashion 2–3 times per week for the development of chronic gait abnormalities and spastic paralysis indicative of demyelination, and assigned a clinical score of 0 to 6 as follows: 0 = asymptomatic, 1 = mild waddling gait, 2 = severe waddling gait, intact righting reflex, 3 = severe waddling gait, spastic hind limb paralysis, impaired righting reflex, 4 = severe waddling gait, spastic hind limb paralysis, impaired righting reflex, mild dehydration, and/or malnutrition, 5 = total hind limb paralysis, severe dehydration, and/or malnutrition, 6 = death. The data are plotted as the mean clinical score for animals from three pooled experiments.

***In vitro* T cell proliferation assays** T cell proliferative responses were assessed by incorporation of [^{3}H]-thymidine. A total of 10^6 viable splenocytes recovered from TMEV infected mice at day 50 p.i. were cultured in triplicate in 96-well, flat-bottom plates in 0.2 ml HL-1 media (Biowhittaker, Walkersville, MD) supplemented with 5% FBS (Sigma, St. Louis, MO), 2 mM glutamine, 100 μg/ml streptomycin, and 100 U/ml penicillin (Gibco BRL, Gaithersburg, MD). A range of VP2 70-86, PLP139-151, and OVA323-339 peptide antigen concentrations (0.1–100 μM final), and 5 μg of UV-inactivated intact TMEV were tested. Plates were pulsed with 1 μCi [^{3}H]-thymidine after 72 h of culture and harvested for scintillation counting on a Packard TopCount plate reader 24 h later. The results are expressed as mean CPM of antigen containing cultures.

Delayed-type hypersensitivity (DTH) DTH responses were quantitated using a standard 24-h ear-swelling assay. Prechallenge ear thickness was determined using a Mitutoyo model 7326 engineer's micrometer (Schlesinger Tools, Brooklyn, NY). DTH responses were elicited by injected 10 μg of peptide (in 10 μl of PBS), or 5 μg of UV-inactivated TMEV into the dorsal surface of the ear using a 100-μl Hamilton syringe fitted with a 30-gauge needle. Twenty-four h after ear challenge, the increase in ear thickness over pre-challenge measurements was determined. Results are expressed in units of 10^{-4} in $\pm$ SEM. Ear-swelling responses were the result of mononuclear

cell infiltration and showed typical DTH kinetics (i.e., minimal swelling at 4 h, maximal swelling 24–48 h).

CNS histology At day 50 p.i., 2 mice from each group were anesthetized and sacrificed by perfusion through the left ventricle with 10 ml of PBS, followed by 100 ml of chilled 3% glutaraldehyde in PBS, pH 7.3. Spinal cords were dissected from the vertebral canal, sectioned at 1-mm intervals, postfixed in 1% osmic acid for 1 h, and processed for Epon embedding. Ten 1-μm-thick sections from each spinal cord were stained with toluidine blue and examined by light microscopy. Pathologic changes were graded in a blinded manner as follows: −, no disease; +/−, meningeal inflammation; +, focal parenchymal inflammation with demyelination; ++, multiple areas of parenchymal inflammation and demyelination; +++, extensive inflammation and demyelination with confluent lesions.

Immunohistochemistry for CD4, CD8, and F4/80 At day 50 p.i., 2 mice from each group were anesthetized and sacrificed by perfusion through the left ventricle with 30 ml of ice-cold PBS. Spinal cords were removed by dissection, and 2–3-mm spinal blocks were immediately frozen in OCT (Miles Laboratories, Elkhart IN) in liquid nitrogen. The blocks were stored at −80°C in plastic bags to prevent dehydration. Then, 5–6-μm-thick sections from the lumbar region (approximately L2-L3) were cut on a Reichert-Jung Cryocut 1800 cryotome (Leica Instruments, Deerfield, IL), mounted on Superfrost Plus electrostatically charges slides (Fisher Scientific, Hanover Park, IL), air dried, and stored at −80°C.

Slides were stained using Tyramide Signal amplification (TSA) Direct Kit (NEN Life Science Products, Boston, MA) according to the manufacturer's instructions. Sections from each group were thawed, air-dried, fixed in acetone at room temperature, and rehydrated in 1× PBS. Nonspecific staining was blocked using anti CD16/CD32 (FcγR II/III-2.4G2, Pharmingen, San Diego, CA), and an avidin/biotin blocking kit (Vector Laboratories, Burlingame, CA) in addition to the blocking reagent provided by the TSA kit. Slides were stained with the following biotin-conjugated antibodies: anti-macrophage (F4/80) (Caltag, Burlingame, CA); anti-CD4 (H129.19), and anti-CD8a (53-6.7) (Pharmingen). Sections were counterstained with DAPI (Sigma) or propidium iodide (Molecular Probes, Eugene, OR), and then coverslipped with Vectashield mounting medium (Vector). Slides were then examined by epifluorescence using a chroma triple-band filter (Chroma Technology Corporation, Brattleboro, VT). Four serial sections from each sample per group were analyzed at 100× and 400× magnification throughout the entire spinal cord section, which included gray and white matter, and dorsal, ventral, and lateral regions.

Plaque assay for viral titer At day 50 p.i., 3–4 mice per group were sacrificed by anesthesia. The brain, spinal cord, and kidney were removed and homogenized in PBS, and diluted in serum-free DMEM to obtain at least three serial dilutions for the assay. BHK-21 cells seeded 2 days prior in 60 × 15-cm tissue culture plates, and grown to confluency, were washed 1× with serum-free DMEM prior to the addition of homogenized tissue dilutions. Infection of the BHK cells is accomplished by incubation of the serial dilutions of homogenate with the cells at room temperature for 1 h with occasional swirling. A sterile 2% top agar solution is added in equal volume to 2× DMEM supplemented with 2% FBS, 5 mM L-glutamine, 200 μg/ml penicillin, and 200 μg/ml streptomycin. After the 1-h incubation, the DMEM/agar mixture is added to the plate and the BHK cells are incubated at 34°C for 6 days in a humidified environment. Following the 6-day incubation, the agar layer is removed and the BHK cells are fixed with methanol. The cells are then stained with a crystal violet solution (6 g crystal violet, 100 ml ethanol, and 400 ml H_2O), and the plaques are visualized on each plate. The number of plaques counted on each plate are multiplied by the homogenate dilution and the amount of homogenate added to the plate to determine the plaque forming units (PFU) per ml. The weight of the original starting tissue (mg) per ml of homogenate is then used to calculate the PFU/mg.

Isolation of RNA At day 50 following induction of TMEV-IDD, two mice from each group were anesthetized and perfused through the left ventricle with 50 ml of PBS. Spinal cords were extruded by flushing the vertebral canal with PBS and then rinsed in PBS. Tissues were forced through a 100-mesh stainless steel screen to give a single cell suspension and pelleted by centrifugation at 1200 RPM for 5 min at 4°C. The pellets were vigorously resuspended in 16 ml of 4 M guanidinium isothiocyanate/50 mM Tris-Cl (pH 7.5)/25 mM EDTA (Gibco BRL); 1% 2-mercaptoethanol. Shearing of DNA was facilitated by forcing the resulting suspension repeatedly through a 23-gauge needle. Total RNA was isolated by high-speed gradient centrifugation (27,000 RPM) of 8 ml lysate through a 3-ml 5.7 M CsCl pad using a SW41 swinging bucket rotor for 20 h at 4°C. The resulting RNA pellet was resuspended to a final concentration of 1 μg/μl with diethylpyrocarbonate (DEPC)-treated water and stored in aliquots at −70°C.

First strand cDNA synthesis and RT-PCR First strand cDNA was generated from 2 μg total RNA using Advantage-RT Kit (Clontech, Palo Alto, CA) using 20 pmole oligo-dT primer as per the manufacturer's provided protocol in a total volume of 20 μl. Following first strand synthesis, each cDNA sample was brought to a final volume of 100 μl with distilled water. Final PCR conditions included 50 mM KCl; 10 mM Tris-Cl (pH 8.3); 2.5–5.0 mM $MgCl_2$ (empirically determined for each primer pair); 2 mM dNTPs; 100 pmoles of each 5′ and 3′ gene-specific primer; 1 U Taq polymerase (Qiagen, Chatsworth, CA) and 5–10 μl diluted cDNA. Cycling conditions were 94°C, 40 s; 60°C, 20 s; 72°C, 40 s, for a total of 30 cycles;

linked to a final 72°C extension program for 3 min and then to a final 4°C soak program. PCR products were run on an ethidium-bromide-containing 2% agarose gel and illuminated using an ultraviolet light source, then photographed using Polaroid type 667 film. Gel images were then scanned into Adobe Photoshop using an Epson 1200-C scanner and imported as TIFF files into Kodak 1D Digital Science for densitometry. The sum intensity and band area were determined for each amplified product and adjusted to each sample's housekeeping gene, HPRT. Data are expressed as a percentage of normalized HPRT expression.

Acknowledgement

This work was supported by USPHS NIH Grant NS-23349.

References

Begolka WS, Vanderlugt CL, Rahbe SM, Miller SD (1998). Differential expression of inflammatory cytokines parallels progression of central nervous system pathology in two clinically distinct models of multiple sclerosis. *J Immunol* **161:** 4437–4446.

Borrow P, Welsh CJ, Nash AA (1993). Study of the mechanisms by which $CD4^+$ T cells contribute to protection in Theiler's murine encephalomyelitis. *Immunology* **80:** 502–506.

Carter L, Dutton RW (1996). Type 1 and type 2: A functional dichotomy for all T cell subsets. *Curr Opin Immunol* **8:** 336–342.

Clatch RJ, Lipton HL, Miller SD (1986). Characterization of Theiler's murine encephalomyelitis virus (TMEV)-specific delayed-type hypersensitivity responses in TMEV-induced demyelinating disease: Correlation with clinical signs. *J Immunol* **136:** 920–927.

Clatch RJ, Melvold RW, Miller SD, Lipton HL (1985). Theiler's murine encephalomyelitis virus (TMEV)-induced demyelinating disease in mice is influenced by the H-2D region: Correlation with TMEV-specific delayed-type hypersensitivity. *J Immunol* **135:** 1408–1414.

Croft M, Carter L, Swain SL, Dutton RW (1994). Generation of polarized antigen-specific CD8 effector populations: Reciprocal action of interleukin (IL)-4 and IL-12 in promoting type 2 versus type 1 cytokine profiles. *J Exp Med* **180:** 1715–1728.

Dethlefs S, Brahic M, Larsson-Sciard EL (1997). An early, abundant cytotoxic T-lymphocyte response against Theiler's virus is critical for preventing viral persistence. *J Virol* **71:** 8875–8878.

Fiette L, Aubert C, Brahic M, Pena Rossi C (1993). Theiler's virus infection of β2-microglobulin-deficient mice. *J Virol* **67:** 589–592.

Friedmann A, Frankel G, Lorch Y, Steinman L (1987). Monoclonal anti-I-A antibody reverses chronic paralysis and demyelination in Theiler's virus-infected mice: Critical importance of timing of treatment. *J Virol* **61:** 898–903.

Gerety SJ, Rundell MK, Dal Canto MC, Miller SD (1994). Class II-restricted T cell responses in Theiler's murine encephalomyelitis virus (TMEV)-induced demyelinating disease. VI. Potentiation of demyelination with and characterization of an immunopathologic $CD4^+$ T cell line specific for an immunodominant VP2 epitope. *J Immunol* **152:** 919–929.

Graves MC, Bologa L, Siegel L, Londe H (1986). Theiler's virus in brain cell cultures: Lysis of neurons and oligodendrocytes and persistence in astrocytes and macrophages. *J Neurosci Res* **15:** 491–501.

Haynes LM, Vanderlugt CL, Dal Canto MC, Melvold RW, Miller SD (2000). $CD8^+$ T cells from Theiler's virus-resistant BALB/cByJ mice downregulate pathogenic virus-specific $CD4^+$ T cells. *J Neuroimmunol* **106:** 43–52.

Inoue A, Koh CS, Yamazaki M, Yahikozawa H, Ichikawa H, Yagita H, Kim BS (1998). Suppressive effect on Theiler's murine encephalomyelitis virus-induced demyelinating disease by the administration of anti-IL-12 antibody. *J Immunol* **161:** 5586–5593.

Kappel CA, Dal Canto MC, Melvold RW, Kim BS (1991). Hierarchy of effects of the MHC and T cell receptor beta-chain genes in susceptibility to Theiler's murine encephalomyelitis virus-induced demyelinating disease. *J Immunol* **147:** 4322–4326.

Karpus WJ, Pope JG, Peterson JD, Dal Canto MC, Miller SD (1995). Inhibition of Theiler's virus-mediated demyelination by peripheral immune tolerance induction. *J Immunol* **155:** 947–957.

Koller B, Marrack P, Kappler J, Smithies O (1990). Normal development of mice deficient in β2-microglobulin, MHC class I proteins and $CD8^+$ T cells. *Science* **248:** 1227–1230.

Kurtzke JF (1993). Epidemiologic evidence for multiple sclerosis as an infection. *Clin Microbiol Rev* **6:** 382–427.

Larsson-Sciard EL, Dethlefs S, Brahic M (1997). *In vivo* administration of interleukin-2 protects susceptible mice from Theiler's virus persistence. *J Virol* **71:** 797–799.

Lavi E, Das Sarma J, Weiss SR (1999). Cellular reservoirs for coronavirus infection of the brain in β2-microglobulin knockout mice. *Pathobiology* **67:** 75–83.

Li L, Sad S, Kagi D, Mosmann TR (1997). CD8 Tc1 and Tc2 cells secrete distinct cytokine patterns *in vitro* and *in vivo* but induce similar inflammatory reactions. *J* Immunol **158:** 4152–4161.

Lin X, Thiemann NR, Pease LR, Rodriguez M (1995). VP1 and VP2 capsid proteins of Theiler's virus are targets of H-2D-restricted cytotoxic lymphocytes in the central nervous system of B10 mice. *Virology* **214:** 91–99.

Lindsley MD, Thiemann R, Rodriguez M (1991). Cytotoxic T cells isolated from the central nervous systems of mice infected with Theiler's virus. *J Virol* **65:** 6612–6620.

Lipton HL, Dal Canto MC (1979). Susceptibility of inbred mice to chronic central nervous system infection by Theiler's murine encephalomyelitis virus. *Infect Immun* **26:** 369–374.

Lipton HL, Gonzalez-Scarano F (1978). Central nervous system immunity in mice infected with Theiler's virus. I. Local neutralizing antibody response. *J Infect Dis* **137:** 145–151.

Lipton HL, Kratochvil J, Sethi P, Dal Canto MC (1984). Theiler's virus antigen detected in mouse spinal cord $2\frac{1}{2}$ years after infection. *Neurology* **34:** 1117–1119.

Matloubian M, Concepcion RJ, Ahmed R (1994). $CD4^+$ T cells are required to sustain $CD8^+$ cytotoxic T-cell responses during chronic viral infection. *J Virol* **68:** 8056–8063.

Miller SD, Karpus WJ (1994). The immunopathogenesis and regulation of T-cell mediated demyelinating diseases. *Immunol Today* **15:** 356–361.

Miller SD, Vanderlugt CL, Begolka WS, Pao W, Yauch RL, Neville KL, Katz-Levy Y, Carrizosa A, Kim BS (1997). Persistent infection with Theiler's virus leads to CNS autoimmunity via epitope spreading. *Nat Med* **3:** 1133–1136.

Murray PD, Pavelko KD, Leibowitz J, Lin X, Rodriguez M (1998). $CD4^+$ and $CD8^+$ T cells make discrete contributions to demyelination and neurologic disease in a viral model of multiple sclerosis. *J Virol* **72:** 7320–7329.

Nicholson SM, Dal Canto MC, Miller SD, Melvold RW (1996). Adoptively transferred $CD8^+$ lymphocytes provide protection against TMEV-induced demyelinating disease in BALB/c mice. *J Immunol* **156:** 1276–1283.

Njenga MK, Pavelko KD, Baisch J, Lin X, David C, Leibowitz J, Rodriguez M (1996). Theiler's virus persistence and demyelination in major histocompatibility complex class II-deficient mice. *J Virol* **70:** 1729–1737.

Ohara Y, Konno H, Iwasaki Y, Yamamoto T, Terunuma H, Suzuki H (1990). Cytotropism of Theiler's murine encephalomyelitis viruses in oligodendrocyte-enriched cultures. *Arch Virol* **114:** 293–298.

Pena Rossi C, McAllister A, Fiette L, Brahic M (1991). Theiler's virus infection induces a specific cytotoxic T lymphocyte response. *Cell Immunol* **138:** 341–348.

Pena-Rossi C, McAllister A, Tanguy M, Kagi D, Brahic M (1998). Theiler's virus infection of perforin-deficient mice. *J Virol* **72:** 4515–4519.

Peterson JD, Karpus WJ, Clatch RJ, Miller SD (1993). Split tolerance of Th1 and Th2 cells in tolerance to Theiler's murine encephalomyelitis virus. *Eur J Immunol* **23:** 46–55.

Pope JG, Karpus WJ, Vanderlugt CL, Miller SD (1996). Flow cytometric and functional analyses of CNS-infiltrating cells in SJL/J mice with Theiler's virus-induced demyelinating disease: Evidence for a $CD4^+$ T cell-mediated pathology. *J Immunol* **156:** 4050–4058.

Pullen LC, Miller SD, Dal Canto MC, Kim BS (1993). Class I-deficient resistant mice intracerebrally inoculated with Theiler's virus show an increased T cell response to viral antigens and susceptibility to demyelination. *Eur J Immunol* **23:** 2287–2293.

Rivera-Quinones C, McGavern D, Schmelzer JD, Hunter SF, Low PA, Rodriguez M (1998). Absence of neurological deficits following extensive demyelination in a class I-deficient murine model of multiple sclerosis. *Nat Med* **4:** 187–193.

Rodriguez M, David CS (1985). Demyelination induced by Theiler's virus: Influence of the H-2 haplotype. *J Immunol* **135:** 2145–2148.

Rodriguez M, Dunkel AJ, Thiemann RL, Leibowitz J, Zijlstra M, Jaenisch R (1993). Abrogation of resistance to Theiler's virus-induced demyelination in $H\text{-}2^b$ mice deficient in $\beta 2$-microglobulin. *J Immunol* **151:** 266–276.

Rodriguez M, Lafuse WP, Leibowitz J, David CS (1986a). Partial suppression of Theiler's virus-induced demyelination *in vivo* by administration of monoclonal antibodies to immune-response gene products (Ia antigens). *Neurology* **36:** 964–970.

Rodriguez M, Leibowitz J, David CS (1986b). Susceptibility to Theiler's virus-induced demyelination. Mapping of the gene within the H-2D region. *J Exp Med* **163:** 620–631.

Rodriguez M, Leibowitz JL, Lampert PW (1983). Persistent infection of oligodendrocytes in Theiler's virus-induced encephalomyelitis. *Ann Neurol* **13:** 426–433.

Rodriguez M, Siegel LM, Hovanec-Burns D, Bologa L, Graves MC (1988). Theiler's virus-associated antigens on the surfaces of cultured glial cells. *Virology* **166:** 463–474.

Rodriguez M, Sriram S (1988). Successful therapy of Theiler's virus-induced demyelination (DA Strain) with monoclonal anti-Lyt-2 antibody. *J Immunol* **140:** 2950–2955.

Sad S, Marcotte R, Mosmann TR (1995). Cytokine-induced differentiation of precursor mouse $CD8^+$ T cells into cytotoxic $CD8^+$ T cells secreting Th1 or Th2 cytokines. *Immunity* **2:** 271–279.

Sad S, Mosmann TR (1995). Interleukin (IL) 4, in the absence of antigen stimulation, induces an anergy-like state in differentiated $CD8^+$ TC1 cells: Loss of IL-2 synthesis and autonomous proliferation but retention of cytotoxicity and synthesis of other cytokines. *J Exp Med* **182:** 1505–1515.

Seder RA, Le Gros G (1995). The functional role of $CD8^+$ T helper type 2 cells (comment). *J Exp Med* **181:** 5–7.

Waksman BH (1995). Multiple sclerosis: More genes versus environment. *Nature* **377:** 105–106.

Welsh CJ, Tonks P, Nash AA, Blakemore WF (1987). The effect of L3T4 T cell depletion on the pathogenesis of Theiler's murine encephalomyelitis virus infection in CBA mice. *J Gen Virol* **68:** 1659–1667.

Yauch RL, Palma JP, Yahikozawa H, Koh CS, Kim BS (1998). Role of individual T-cell epitopes of Theiler's virus in the pathogenesis of demyelination correlates with the ability to induce a Th1 response. *J Virol* **72:** 6169–6174.

Zijlstra M, Bix M, Simister NE, Loring JM, Raulet DH, Jaenisch R (1990). Beta 2-microglobulin deficient mice lack $CD4^-8^+$ cytolytic T cells. *Nature* **344:** 742–746.